Computer Assisted Methods in Engineering and Science, **23**: 147–166, 2016.
Copyright © 2016 by Institute of Fundamental Technological Research, Polish Academy of Sciences

Multi-objective model-based design optimization of hydraulic shock absorbers

Grzegorz Wszołek
Silesian University of Technology
Institute of Engineering Processes Automation and Integrated Manufacturing Systems
Konarskiego 18a, 44-100 Gliwice, Poland
e-mail: grzegorz.wszolek@polsl.pl

This paper presents the multi-objective optimization process of a hydraulic damper design based on its interdisciplinary meta-model considering both the properties of a damper and of the testing equipment used for the purpose of design criteria verification, and in particular the tolerance band criterion of damping force characteristics, the criterion of maximum permissible vibration level expressed with the piston rod acceleration and the criterion of fatigue durability for the damper's hydraulic valve system. The meta-model of a damper and a testing bench include the following models: mechanical model, hydraulic model, electro-hydraulic model and valve system fatigue durability model. The multi-objective optimization method provides an optimal solution by means of Pareto frontier. Furthermore, all potential feasible solutions are ranked according to additional customer preferences to select the most suitable ones. The proposed method is intended to be used to determine the best starting point in a new shock absorber design process.

Keywords: multi-objective optimization, model-based design, shock absorber model.

1. Introduction

Recently, the model-based design (MBD) approach has been frequently used in order to find the best starting point for the design validation process without using physical parts and prototypes. The MBD approach allows overcoming the difficulties of traditional development process using comprehensive, system-level mathematical models that serve as executable specifications and product know-how repository. Engineers can simulate and iterate as many times as necessary to refine the model to meet the constraints of the target product, and to validate the product behavior against the requirements of building risk assessment scenarios or optimizing specific product properties. The MBD facilities ensure quality throughout the development process by integrating tests into the product development process at any stage. This continuous small-step improvement and validation provide a better understanding of the prototype design. Another advantage is early identification of error and contradictory requirements before any physical prototypes are machined and run through series of expensive tests. The MBD top-level approach is to consider contradictory design features to achieve the optimal trade-off among customer requirements, available manufacturing capabilities, design and manufacturing costs. The fundamental challenge in the design of automotive shock absorbers is to find a trade-off among the damping force, noise vibration and harshness (NVH) and durability performance requirements. This paper highlights the optimization method that has a potential to advise the engineers on how to meet the customer specifications. The damping force performance is the damping force specification given at specific piston rod assembly velocities [1]. The damping forces have a specific tolerance band that defines the boundary condition acceptable by the customer. An NVH performance is evaluated using a diagram of vibration amplitude in

the specific frequency range considered by a vehicle manufacturer. Lastly, the fatigue durability performance is the shock absorber lifetime until any failure or performance deterioration occurs.

2. State of the research on shock absorber modelling

Shock absorber models are rarely used in design optimization regarding combined multi-domain requirements, e.g., damping-force, vibration level, and durability. Most of the presented optimization problems deal with a single objective optimization of particular systems of shock absorbers, e.g., valve system. Wang et al. [2] conducted a comprehensive optimization of the valve system of the adjustable shock absorber with respect to both technical and economic criteria. A multi-objective model for design optimization was formulated in order to optimize both technical and economic capabilities of a complete three-valve system in a shock absorber, based on a complete physical damper model. Nevertheless, the reduction to a single-objective optimization was problematic and for that reason the weighted criterion method had to be used [2]. The simulation results showed that the optimal result met all the competing objectives well within the constraints, with the exception of some minor and tolerable compromises in the response performance of the relief valve. On the other hand, a prototype experimental work proved that the prototype dampers have presented exemplary damping characteristics [2]. Kaldas [3] proposed a new methodology for the optimization of the damper top mount characteristics and to increase driving comfort and reduce harshness. He developed a combined objective function that includes ride comfort, harshness, and impact harshness evaluations, and he used it in the optimization routine. In addition, a precise mathematical model of a damper top mount was implemented inside a quarter vehicle model in order to produce accurate simulation results for the optimization study [3]. Satpute [4] discusses mathematical modeling of the fluid damper that uses a number of shim controlled orifices. A finite element analysis (FEA) is performed to compute stiffness of the shims used with the orifice, while the pressure difference and damping force across the piston using fluid flow continuity equations is obtained. Finally, a single-degree-of-freedom (SDOF) damper model is used to find displacement transmissibility for the specific range of frequencies [4]. Sonnenburg [5] concluded that engaging a conservative force element in the damper module results in higher driving safety and decreases driving comfort (measured in root mean square- RMS values). This is a very surprising result since it is believed that the top mount is only needed for comfort. Sonnenburg concluded [5] that it is possible, depending on the excitation, to minimize the dynamic wheel load fluctuation up to 20% using a pure damper instead of a damper module. The damper module provides driving safety at the same comfort level. Sonnenburg developed a very simple method of finding the optimal combination of parameters for the damper module as compared to the existing methods [5]. A key challenge for chassis designers is selecting the relevant excitation that satisfies their expectations for future use of the car. But in the case of today's tuning process, test side roads turn out to be very helpful in this respect. They need to be analyzed in terms of their amplitude spectrums, and then they are put into the proposed cost function [5]. Following the latest research, one can notice that the shock absorber studies and analyses regarding durability [6] and vibration in the frequency ranges up to 700 Hz [7, 8] have still potentials to be further researched. Nevertheless, the current state of the shock absorber research shows that these methods developed sufficiently accurate and versatile models to represent the physical units in damper design process. It is therefore feasible to use them in the optimization process. The formalized method of finding the optimal shock absorber configuration regarding design parameters is not yet known.

Wszołek et al. [9] have proposed and developed a method of determining an objective assessment of a shock absorber regarding vibrations by means of piston-rod acceleration measurements. This method requires laboratory testing component on the shock absorber system, which is isolated from the rest of the vehicle, with servo-hydraulic test systems that repeatedly simulate road conditions. The proposed approach allows eliminating interactions between the shock absorber and the suspension elements of the vehicle; component tests also allow for quantification of noise and vi-

bration characteristics of the damper by measuring the vibration acceleration of the housing of the shock absorber and its piston rod. The outcome of practical realization of this approach is the need to consider the impact of dynamic testing machine on amplitude-frequency response of a shock absorber. The study showed that this impact covers the frequency range of up to about 700 Hz, depending on the geometric and physical properties of a shock absorber [9, 10]. The proposed multi-objective optimization method, due to a wide scope of analysis in the sense of considered frequency band, requires taking into account the susceptibility of a mechanical-hydraulic test system (usually the laboratory) used to excite vibrations of the shock absorber. The developed methods use advanced multidisciplinary simulation of a nonlinear shock absorber model and testing system model [9]. Identification of the model's ability to estimate the parameter values is carried out using experimental measurements [10]. Wszołek et al. [11] have applied a single-objective optimization method in order to minimize vibrations of a shock absorber. The model-based approach was proposed to obtain the optimal pressure-flow characteristics by simulations conducted with the use of coupled models including the damper and servo-hydraulic tester model. Two alternative optimization methods, namely a function response surface (FRS) method [12, 13] – a 'quick-and-dirty' method and a nonlinear programming (numerical optimization) method were proposed. The FRS is supported with a design of experiment (DoE) plan and a simulation model including relevant physical phenomena in order to study valve design physical properties. The method is based on the linearly approximated solution that, in specific circumstances, can deliver less accurate results, but in shorter time. Lower accuracy can be a case if an optimization parameter space exhibits highly nonlinear relationships that cannot be well approximated by the linear regression. However, the FRS method shortens computation time compared to the nonlinear programming method [14, 15]. On the other hand, the nonlinear programming is sensitive to the selected optimization technique, initial conditions, algorithm settings and drawbacks such as local minima occurring during the convergence process of the algorithm. Therefore, a nonlinear programming method requires advanced knowledge that is not always available among the engineering staff. The invented laboratory methods presented in [16, 17] were used in order to support the model validation tests.

3. Meta-model applied to optimization process

This paper presents the architecture of the shock absorber meta-model and briefly describes each component of the model. The model allows reproducing experimental and operational conditions. The meta-model presents a combination of first-principle models (distributed finite element model and lumped parameter model) and black-box interpolated formulas in the form of look-up tables. The model combines a shock absorber model, a test-rig model and valve durability fatigue model.

3.1. Hydraulic shock absorber model

The considered hydraulic shock absorber corresponds to a typical design of a monotube shock absorber commonly used in passenger or commercial vehicles [1]. The hydraulic shock absorber uses a piston traveling within a single tube that is exposed more directly to the air facilitating cooling during high-speed or longer tests. To prevent foaming and bubble formation in the oil, which degrade the force performance during longer tests, a gas-filled chamber of high-pressure gas is located in parallel to the oil chamber. This high-pressure gas makes it difficult for bubbles to form in the oil. The compression gas chamber allows also to compensate the change in the upper compression and rebound chambers caused by the moving up-and-down piston-rod assembly, and thermal expansion of the oil due to an increase of temperature. A typical single-tube hydraulic shock absorber is shown in Fig. 1.

The side of the piston attached to the rod is referred to as the rebound volume. The side with the larger area is the compression volume [1]. Oil occupies the tube volume on either side of the piston. The shock absorber has a moving separator (floating piston) within the tube volume across

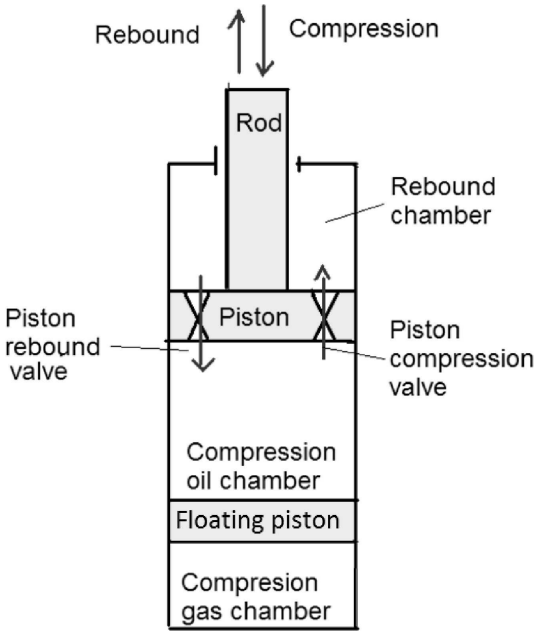

Fig. 1. Hydraulic shock absorber working principle.

from the head side of the piston. The additional piston separates the oil from a volume of gas under pressure (approximately 5–30 bars). During the compression stroke (the rod moves inside the tube), the hydraulic fluid from the head side volume is forced through an arrangement of valves and orifices across the piston and into the rod-side volume. First, the oil enters any of several port restrictions when the pressure differential across the check valve exceeds a preset value. The fluid then enters a small junction volume within the piston before passing to the other side of the piston through a set of orifices referred to as the bleed leak restrictions. A second conduit opens from the junction volume to the other side of the piston through pressure relief valve when the pressure differential exceeds a preset value. Oil can also leak around the gap between the piston seal and the tube inner diameter. The relative incompressibility of oil and the fact that the displaced volume on the head side is larger than that of the rod side result in a reduction of gas volume to account for the additional volume of fluid on the head side, which could not be forced to the rod side. During rebound stroke, the fluid on the rod side increases in pressure relative to the head side and the oil flows across the piston to the head side through a separate set of ports and orifices than those active on the compression stroke. The compression ports are closed-off by a system of check valves during the rebound stroke and vice versa. However, as opposed to the compression stroke, the nitrogen gas volume provides compensation for a decreasing oil volume. The hydraulic shock absorber nonlinearities are related to a variable oil volume, friction of the main and floating piston, nonlinear valve characteristics, and the gas and fluid model.

The model of a hydraulic shock absorber introduced in this section is formulated and discussed in [10]. The proposed model formulation facilitates the inclusion of the oil-gas emulsion model [1]. The presented hydraulic shock absorber model has been developed based on the following assumptions:

- dependency between density and pressure is nonlinear (oil-gas emulsion),
- pressure and density are uniformly distributed in particular chambers,
- pressure-flow characteristics of all restrictions are given as monotonic functions,
- valves open and close abruptly in a completely symmetrical manner (valve dynamics is not considered),

- oil temperature is constant,
- friction between floating piston and pressure tube is neglected (friction is small compared to other frictions because of low friction sealing and lack of side force),
- mass of floating piston is neglected because it is few times smaller than oil mass thus inertia is also neglected.

The model parameters used in this paper are presented in Table 1.

Table 1. Parameters of the hydraulic shock absorber model.

Configuration parameters	Values
Bulk modulus of an oil K	1.6e9 [N/m^2]
Ratio of the gas/oil mass ζ	1e-8 [–]
Gas constant (nitrogen) R	8.31 [J/(mol/K)]
Oil temperature T	309[K] (≈36 [°C])
Total oil volume V_{oil}	6.3814e-004 [m^3]
Moving mass m_1 (top mount + piston-rod assembly mass)	1.5 [kg]
Initial gas pressure p_{ini}	5e5 [Pa]
Area of the rod section A_{rod}	9.5033e-005 [m^2]
Area of the piston section A_{com}	100e-5 [m^2]
Initial volume of the rebound chamber $V_{\text{reb\_ini}}$	1.2920e-004 [m^3]
Initial volume of the compression chamber $V_{\text{com\_ini}}$	5.0894e-004 [m^3]

3.2. Servo-hydraulic test-rig model

Vibration evaluation is performed on the entire vehicle under road and laboratory conditions. However, it is also frequently performed on isolated systems of gradually increasing complexity in laboratory conditions, i.e., suspension or hydraulic shock absorber level. This approach allows for interactions with the vehicle body to be eliminated and then, in turn, for test conditions to be more precisely controlled. Laboratory experiments are more repeatable than on-road driving sessions. It is also easier to simulate typical road maneuvers and measure certain signals such as tire forces, or use special measurement equipment. On the other hand, laboratory-based tests enable the reduction of costs and allow for tests to be performed faster. Vibration tests performed on a servo-hydraulic tester are intended to quantify and rank the intensity of vibrations generated by hydraulic shock absorbers [7]. The servo-hydraulic tester affects the evaluation of test results since the hydraulic actuator has a variable stiffness and specific resonance frequency. It is therefore necessary to include the servo-hydraulic tester dynamic by means of its model coupled to the hydraulic shock absorber model.

The model of a servo-hydraulic test rig used in this study was the model developed in [7, 10]. The servo-hydraulic installation is equipped with accumulators providing separation between gas and liquid volumes using an elastic diaphragm or a floating piston, therefore it is adequate to use volumetric flow balance instead of mass-flow balance. In turn, oil properties are assumed to be unaffected by the presence of gaseous fraction in the oil and significant changes in the oil bulk module. The model assumes constant oil temperature. The behavior of a hydraulic shock absorber connected with a top-mount is described by the model whose equations were precisely developed in [10].

The hydraulic shock absorber and the servo-hydraulic tester models are coupled via force, velocity and displacement feedback relationships as presented in [7]. A hydraulic shock absorber is

rigidly attached to the main frame of the servo-hydraulic tester through a top fixation (the load cell) and a top mount. The bottom end is rigidly connected to the rod of the hydraulic actuator. The servo-tester model parameters are introduced in Table 2.

Table 2. Parameters of the servo-hydraulic tester model.

Configuration parameters	Values
Proportional (P)	0.052
Integral (I)	0.1
Derivative (D)	0
Feed-forward (FF)	0
Fluid bulk modulus	1.5e9 [N/m^2]
Piston rod diameter	45 [mm]
Volume chamber A and B	93.2e-6 [m^3]
Area of piston side A and B	373 [mm^2]
Piston mass	10 [kg]
Oil temperature T	309[K] (≈36 [°C])
Piston friction	10 [Ns/m]
Chamber leak rate	10e-6 [cm^3/s]

The equivalent system of the servo-hydraulic tester is formulated as a serial connection of mass, damping, and stiffness equivalent elements [7, 18]. In this model, the coefficients representing damping and stiffness of a hydraulic shock absorber and a hydraulic actuator are nonlinear, and their values result from the nonlinear hydraulic flow equations presented in the previous sections. The model requires a few physical parameters, which are related to fluid (oil) properties affected by ambient conditions, e.g., oil density.

Other model physical parameters are provided in the form of parameters and characteristics, such as top mount stiffness or piston friction respectively. The fixed geometrical parameters are measured directly or taken from the customer specifications regarding the hydraulic actuator. The last category consists of the phenomenological parameters to which hydraulic leakages, gas/oil mass ratio, discharge and piston friction coefficients belong [19]. These parameters are known only by their approximate values obtained at specific conditions, e.g., fixed ambient temperature. Hydraulic leakages over the piston are difficult to obtain without precise measurements due to unknown tube-piston tolerances. Leakages over the piston-rod assembly in hydraulic shock absorbers are tunable and controlled using valve discs with calibrated orifices. The gas-oil mass ratio was roughly calculated using Henry's equation [1], while the critical discharge coefficient of the servo-valve is a free parameter. A top-mount is an external component attached to the shock absorber, which transfers the rod force to the suspension. Its stiffness is obtained on a static load frame machine as a force-displacement characteristic. The damping and stiffness characteristics of the top-mount were obtained in [10]. The servo-hydraulic tester model uses a simplified model of a servo-valve reduced to the second-order transfer function representing the dynamics of the spool. The transfer function has two parameters, which are the natural frequency and damping ratio obtained in [19].

3.3. Valve system fatigue durability model

A durability model of a shock absorber valve system [20, 21] consists of three sub-models (Fig. 2): (i) first-principle mechanical (stress/strain) finite element model, (ii) experimental lumped-parameter flow model, (iii) experimental fatigue mode, where the mechanical model features: (i) stress in discs, and (ii) displacement between an orifice and a valve seat, both in function

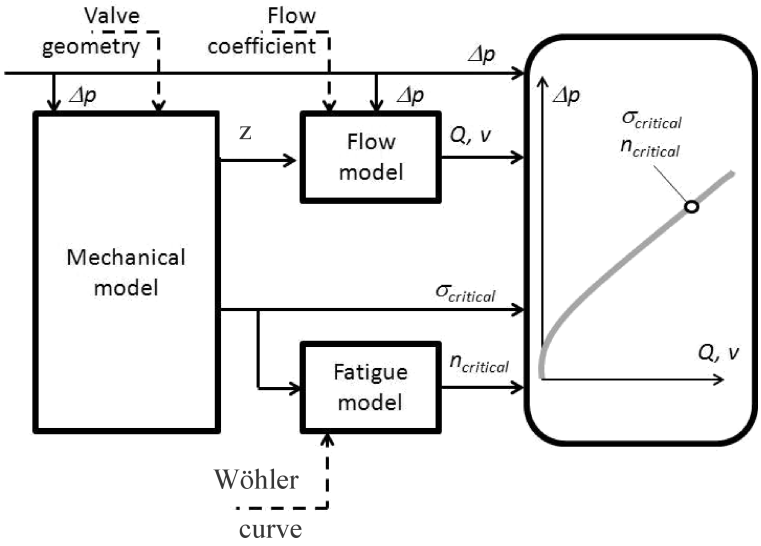

Fig. 2. Valve system fatigue durability model.

of the pressure load. Opening of a disc stack can also be expressed as a function of an outflow area vs. pressure load. If the dashpot geometry is known, the flow model allows for obtaining the outlet flow rate in the valve system in function of the pressure load. The fatigue model obtains a number of cycles withstood by a valve system in function of a stress level. The input of the mechanical model is a pressure drop across the valve system (Δp), while the outputs are the critical stress (σ_{critical}) and the displacement of a disc stack over the valve seat (z). The input to the flow model is the pressure drop (Δp) and the opening displacement (z), while the output is the flow rate or velocity (Q, v).

The complete procedure of a valve system durability evaluation consists of a few steps. In the first step, the pressure-displacement (PD) and pressure-stress (PS) characteristics are obtained based on the known bill of material (BOM) with the use of the mechanical finite element model [22]. If the valve system geometry and the flow coefficient are known, the PD characteristics are converted into the pressure-flow (PQ) characteristics with the use of the flow model. If the flow coefficient is unknown, the PQ characteristics are adjusted in order to minimize errors between the available flow characteristics of the valve system measurements and the model prediction. The stress values are important for assessing the valve system durability. Bending, shear and compound stress can be extracted from the mechanical model. The location where the stress achieves the maximal value needs to be determined. This maximal stress limit is considered in the further durability analysis. Moreover, the mechanical model provides the average disc stack opening height, which is required as an input by the flow model. The disc stack opening regulates the oil flow rate through a valve system, thus determining the damping force. The equal stress lines obtained from the mechanical model are imposed on the pressure or damping force characteristics vs. flow or rod velocity obtained from the flow model.

This enables plotting the iso-stress lines (the lines of equal stress) that pass through the points of equal stress level intersecting the flow/rod velocity lines. Location of the iso-stress lines allows the ride-work engineer to evaluate the criticality of different valve settings. For a given setting (flow-displacement curve), engineer can choose the disc stack that has minimum stresses. Experimentally determined Wöhler curve is required for that purpose. A stress domain is converted into fatigue domain using the set of Wöhler curves in function of a thicker (weaker) disc in a disc stack. Critical stress corresponds to critical damage that causes disc stack failure (crack, deformation). A durability model is coupled with hydraulic damping force model though the piston valve flow characteristics (Fig. 2). The piston valve consists of a stack of thin disc springs of varying diameters, which are designed to provide a controlled annular flow through a valve system [20]. A disc spring stack is subjected to fatigue damage, and therefore it has to be accurately designed and validated to

provide the required fatigue damage performance and minimize failure risk of a shock absorber. The durability model obtains maximal stress in both piston valves, namely rebound and compression. Finally, the most critical valve is the one with highest local stress, which is further considered as the critical stress determining shock absorber life-time. The valve durability model is represented by the set of nonlinear Eq. (1) that require to be solved in respect of the input variable, i.e., the pressure drop across the piston valve assembly. The model uses the following simulation and experimental static functions, which can have parametric or nonparametric representation:

$$\begin{aligned} z &= f_{\text{sim}}(\Delta p, z_0), \\ q_{\text{piston}} &= f_{\text{sim}}(\Delta p, z, \gamma) \quad \text{or} \quad q_{\text{piston}} = f_{\text{exp}}(\Delta p), \\ \sigma &= f_{\text{sim}}(p, z_0), \\ n &= f_{\text{exp}}(\sigma), \end{aligned} \tag{1}$$

where Δp is the differential pressure across the piston valve, namely the difference between the fluid pressure in the rebound and compression chamber, σ is the maximal critical stress occurring in a disc spring, z is the valve opening gap between the first sealed disc spring and the valve port (seat), z_0 is the initial disc spring deformation (i.e., the disc spring preload), n is the number of cycles withstood by a disc stack, q is the flow rate, and γ is the flow coefficient. The flow rate q can be obtained by means of simulation or experimental measurements [20]. The mechanical model requires additional initial conditions to solve the system of equations, namely the preload z_0 of the disc spring stack expressed as the displacement resulting from the assembly torque specification [20]. The critical stress $\sigma_{\text{critical}} = \max(\sigma)$ refers to the conditions where the valve fatigue performance is equal to the boundary conditions of the disc spring failure risk, e.g., crack, plastic deformation.

4. Multi-objective optimization

Modern optimization methods, sometimes also called nontraditional optimization methods, have emerged in recent years as efficient and reliable methods for solving complex engineering optimization problems. These methods include genetic algorithms, simulated annealing, particle swarm optimization, ant colony optimization, neural network-based optimization, and fuzzy optimization. The multi-objective optimization (MOO) is performed for continuous, discrete and binary design variables under the consideration of design and manufacturing constraints. Multiple [23] objective functions including multiple terms and weights are defined from engineering principles. Optimization for solving multi-objective optimization problems has been established for practical applications [23]. The main advantage of the population-based approaches is the parallel search for a set of Pareto-optimal solutions in a single optimization run. In these methods, the fitness function is assigned using Pareto strength ranking, and diversity is preserved by density estimation. Furthermore, dominance-based constraint handling is used. In case of conflicting objectives calculation, visualization and investigation of the set of Pareto optimal solutions provide the basis for deciding which of the designs could be foreseen for production. In order to select one solution from the Pareto front, posterior preferences have to be defined and evaluated along the Pareto frontier (Fig. 3).

The Pareto frontier or Pareto set is the set of parameterizations (allocations) that are all Pareto efficient. Finding Pareto frontiers is needed to find the most relevant design features. By yielding all of the potentially optimal solutions, a designer can make focused trade-offs within this constrained set of parameters, rather than being required to consider full ranges of parameters. Before starting Pareto optimization the detection of conflicting objectives using sensitivity analysis and/or single objective weighted optimization is recommended [24]. Consideration of best designs out of sensitivity analysis and single-objective optimization runs in the start population significantly improves the Pareto optimization performance. The single-objective optimization problem concerning the NVH performance of a hydraulic shock absorber was addressed in [25]. In the weighting method (WM),

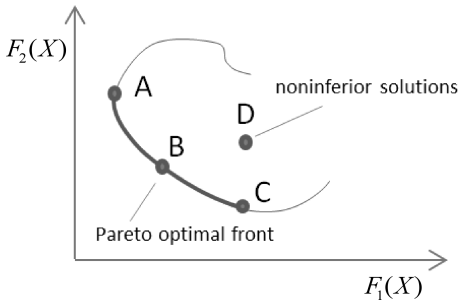

Fig. 3. Pareto frontier.

the objective function (in the vector form) is converted to a scalar by expressing it as weighted sum of the various objectives by associating relative weight to each objective function:

$$F(X) = w_1 \cdot F_1(X) + w_2 \cdot F_2(X) + ... + w_m \cdot F_m(X), \tag{2}$$

$$\begin{aligned} g_i(X) &\leq 0 \qquad i = 1, 2, \ldots, s_1, \\ l_i(X) &= 0 \qquad i = 1, 2, \ldots, t_1, \end{aligned} \tag{3}$$

where X is an n-dimensional vector called the design vector, $F(X)$ is called the objective function, and $g_i(X)$ and $l_i(X)$ are known as inequality and equality constraints, respectively. The number of design variables n and the number of constraints s_1 and/or t_1 do not need be related in any way [23]. Relative weights w reflect the trade-off or the marginal rate of transformation of pairs of objective functions [24]. Weights imply value judgments. These weights are varied systematically and solution is obtained for each set. Solution obtained for a set of weights gives one generated set of non-inferior or efficient solution plans (Fig. 4).

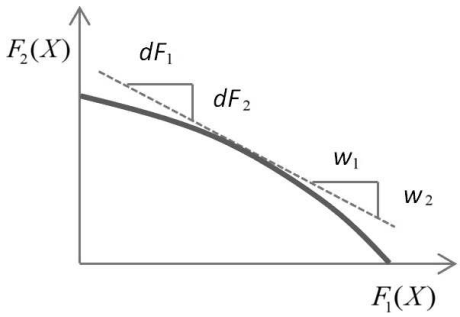

Fig. 4. Weighted single-optimization method.

The range of efficient solutions that cannot be identified with the weighted single-objective optimization is presented in Fig. 5.

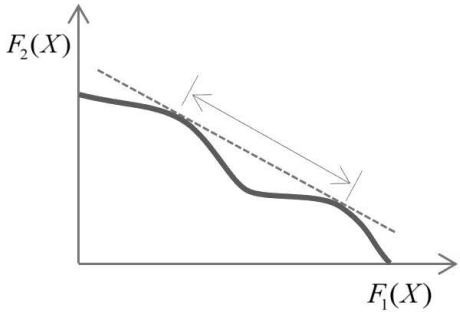

Fig. 5. Range of efficient solutions that cannot be identified with the weighted single-objective optimization.

The major limitation of weighting approach is that it cannot generate a complete set of efficient plans unless the Pareto front is strictly convex [24]. The efficiency frontier between two objectives $F_1(X)$ and $F_2(X)$, showing the reduction in one objective, gives $F_1(X)$, as the relative weight, w_2, associated with the other objective, increases [24]. MOO methods are not intended to identify the best solution, but only to provide information on the trade-offs between considered sets of quantitative performance criteria. The important steps in MOO are [24]:

- plan selection aimed at generating the non-inferior set of solutions (or the set of technologically efficient solutions),
- selecting the best compromise solutions with the weighting or constrain method.

A plan X dominates all other plans if it results in an equal or superior value for all objectives, and at least one objective value is strictly superior to those of each other plan. Non-inferior, efficient, or non-dominated solutions improve the value of any single objective, thus one should have to accept a diminishment of at least one other objective. MOO is concerned with the minimization of a vector of objectives $F(X)$:

$$\min_{x \in R^n} F(X), \tag{4}$$

where

$$F(X) = [F_1(X), F_2(X), ..., F_m(X)], \tag{5}$$

where m denotes the number of objective criteria, and X is an n-dimensional design vector:

$$X = \begin{bmatrix} x_1 \\ x_2 \\ \vdots \\ x_n \end{bmatrix} \tag{6}$$

and $F(X)$ is subjected to the constraints or bounds:

$$\begin{aligned} g_j(X) &\le 0 \qquad j = 1, 2, \ldots, s_2, \\ l_j(X) &= 0 \qquad j = 1, 2, \ldots, t_2, \end{aligned} \tag{7}$$

where X is an n-dimensional vector called the design vector, $F(X)$ is called the objective function, and $g_j\ (X)$ and $l_j(X)$ are known as inequality and equality constraints, respectively. The number of variables n and the number of constraints s_2 and/or t_2 do not need to be related in any way [23]. The optimization result is the set of Pareto feasible solutions available in the m-th order multidimensional space as follows:

$$P(X) = \begin{bmatrix} F_{1,1}(X) & F_{1,2}(X) & \ldots & F_{1,m}(X) \\ \vdots & \vdots & & \vdots \\ F_{r,1}(X) & F_{r,2}(X) & \ldots & F_{r,m}(X) \end{bmatrix}, \tag{8}$$

where r is the number of considered Pareto feasible solutions. The Pareto solutions representing individual rows of P matrix are further ranked regarding subjective criteria, which represent "soft" engineering knowledge and customer preferences, e.g., importance of fatigue performance over damping force tolerance limits. The Pareto solutions ranking is obtained using a Minkowsky distance metric between each vector of particular feasible solutions and the reference solution:

$$P_0 = \begin{bmatrix} F_{0,1} & F_{0,2} & \ldots & F_{0,m} \end{bmatrix}, \tag{9}$$

where F_0 denotes assumed, simulated, or measured values of optimization criteria. A similar shock absorber design can be considered as a reference solution. Otherwise, the so-called "utopia point" corresponding to the origin of a design parameters' space under assumption of minimization objective functions is assumed to be a reference solution, i.e., $F_{0,1} = 0$, $F_{0,2} = 0$, ..., $F_{0,r} = 0$. Minkowsky distance metric input data is given as an r-by-m data matrix F containing evaluated objective functions for particular design vectors and a 1-by-m data matrix P_0 containing a reference point. Output data is a following distance vector D, which contains the Minkowsky measures of the considered Pareto optimal solutions:

$$D = \sum_{i=1\ldots r} \left(\sum_{j=1\ldots m} |P_{i,j} - P_{0j}|^c \right)^{1/c}, \tag{10}$$

where c is an arbitrary scalar positive value which for the special case of $c = 1$, the Minkowski metric gives the city block metric, for the special case of $c = 2$, the Minkowski metric gives the Euclidean distance, and for the special case of $c = \infty$, the Minkowski metric gives the Chebychev distance [9].

5. Model-based optimization

MOO demonstration is presented in this paper toward the trade-off among the fundamental hydraulic shock absorber performance criteria which are as follows (Table 3) [25]:

- damping force to meet the customer specification,
- minimized vibrations transfer (NVH),
- maximized lifetime.

In that respect, three objectives functions were formulated: (i) damping force, (ii) vibration level, and (iii) critical stress, as the error metric between the target and actual value. The damping force characteristic refers to a shock absorber force in rebound and compression direction for a specific range of velocities, e.g., up to 1.5 m/s.

Table 3. Optimization parameters.

	Damping force [N]	Acceleration [dB]	Stress [N/m^2]
Target value	Tables 4 and 5	0	0
Acceptable target value	Tables 4 and 5	3 dB lower than initially measured	1600
Improvement direction	↕	↓	↓

The force has to meet specific high-and-low tolerance limits, which are defined by a customer as presented in Tables 4 and 5, and graphically in Fig. 6.

Table 4. Rebound damping force vs. velocity.

Index v	Rebound velocity [m/s]	Rebound force min [N]	Rebound force nominal [N]	Rebound force max [N]	Tolerance [%]
1	0.13	180	200	220	15
2	0.26	263.7	293	322.3	15
3	0.39	336.6	374	411.4	15
4	0.52	408.6	454	499.4	15
5	1.05	706.5	785	863.5	15
6	1.57	1036.8	1152	1267.2	15

Table 5. Compression damping force vs. velocity.

Index v	Compression velocity [m/s]	Compression force min [N]	Compression force nominal [N]	Compression force max [N]	Tolerance [%]
1	0.13	−320.4	−356	−391.6	15
2	0.26	−513.9	−571	−628.1	15
3	0.39	−642.6	−714	−785.4	15
4	0.52	−751.5	−835	−918.5	15
5	1.05	−1193.4	−1326	−1458.6	15
6	1.57	−1667.7	−1853	−2038.3	15

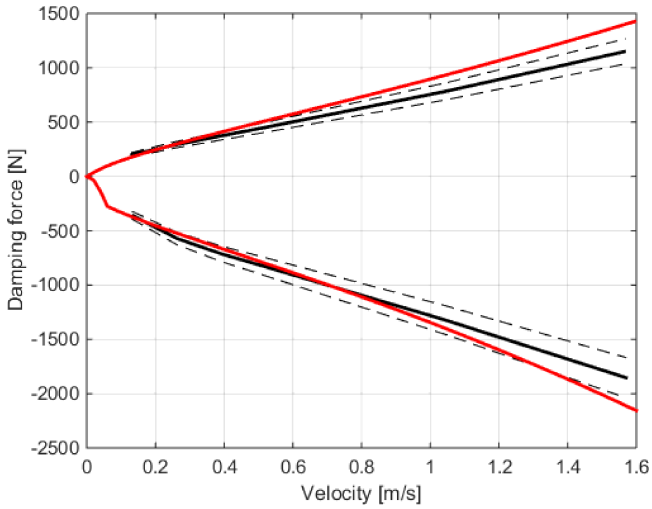

Fig. 6. Damping force performance characteristics.

A typical tolerance limit is 15%. The following error formula is used to obtain the rebound and compression error parts respectively:

$$\varepsilon_{DF} = \frac{1}{2 \cdot k}\left[\sum_{v=1\ldots k}\left(\frac{F_v - F_{\max,v}}{\beta_v}\right)^{\alpha} + \sum_{v=1\ldots k}\left(\frac{F_v - F_{\min,v}}{\beta_v}\right)^{\alpha}\right], \tag{11}$$

where

$$\beta_v = F_{\max,v} - F_{\min,v}, \tag{12}$$

where v is the rebound and compression shock absorber velocity index corresponding to velocities in Tables 4 and 5, k is the maximum number of considered velocities $k = 6$ [–], $F_{\max}$ is the upper bound of the damping force tolerance range [N], $F_{\min}$ is lower bound of the damping force tolerance range [N], β is the damping force tolerance range [N], and α is the error metric exponent assumed as a linear distance metric $\alpha = 1$.

The noise of a shock absorber includes friction noise, air current noise, liquid current noise and structural noise [1]. Research work and experiments indicate that abnormal noise is related to high-frequency vibration ranging from 100 to 700 Hz on the piston rod assembly, during the alternation of rod travel direction [1]. The NVH objective function is defined as an average mean square error between the target and actual PSD characteristics (Fig. 7) in the specific frequency range ($a = 70$ Hz, $b = 400$ Hz, step = 10 Hz), as follows:

$$\varepsilon_{\text{PSD}} = \left|\frac{1}{b-a}\sum_{f=a\,:\,\text{step}\,:\,b}\left[\operatorname{sgn}\left(A_f - A_{\text{ref},f}\right) * \left(\frac{A_f - A_{\text{ref},f}}{\text{tol}_{\text{PSD}}}\right)^{\alpha}\right]\right|, \tag{13}$$

where f is the index of PSD frequencies distributed with a step = 10 Hz over the analyzed frequency range (a = 70 Hz, b = 400 Hz) and $f = \{70, 80, \ldots, 400\}$, tol_{PSD} is the tolerance coefficient assumed to be tol_{PSD} = 2 dB, A is the vibration amplitude $10\log_{10}(\cdot)$ [dB], A_{ref} is the reference vibration amplitude $10\log_{10}(\cdot)$ [dB], and α is the error metric exponent assumed as a linear distance metric $\alpha = 1$.

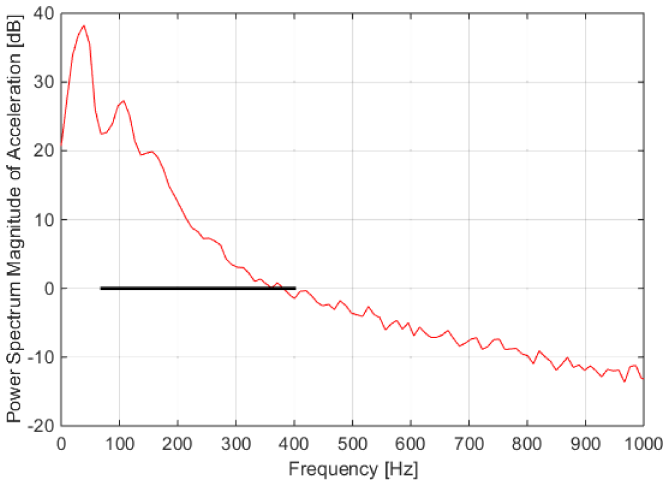

Fig. 7. Damping force performance characteristics.

Fatigue durability objective function represents the difference between the critical and calculated stress in a disc valve system. The stress is the maximal stress of one of the discs in a disc stack, typically at the thickest ones [10]. The reference stress σ_{ref} = 0 [MPa] is assumed in case if optimization runs are performed for a new valve systems and this case is considered in the paper, otherwise a reference stress is set as 20% less than the reference stress of the similar disc stack. The following error formula is used to obtain the rebound and compression stress components respectively:

$$\varepsilon_S = \left| \frac{1}{N} \sum_{v=1\ldots k} \left[\text{sgn}\left(\sigma_v - \sigma_{\text{ref},v}\right) * \left(\frac{\sigma_v - \sigma_{\text{ref},v}}{\text{tol}_{\text{STRESS}}} \right)^{\alpha} \right] \right|, \tag{14}$$

where v is the rebound and compression shock absorber velocity index, i.e., v_1 = 1.5 m/s, v_2 = 2.0 m/s, v_3 = 2.5 m/s, k is the maximum number of considering velocities k = 3 [–], $\text{tol}_{\text{STRESS}}$ is the tolerance coefficient equal to 100 [MPa], σ is the maximum valve stress value [MPa], σ_{ref} is the reference valve stress value [MPa], and α is the error metric exponent assumed as a linear distance metric α = 2. The stress value is obtained at three operational shock absorber velocities, i.e., 1.5, 2.0, 2.5 m/s (Fig. 8).

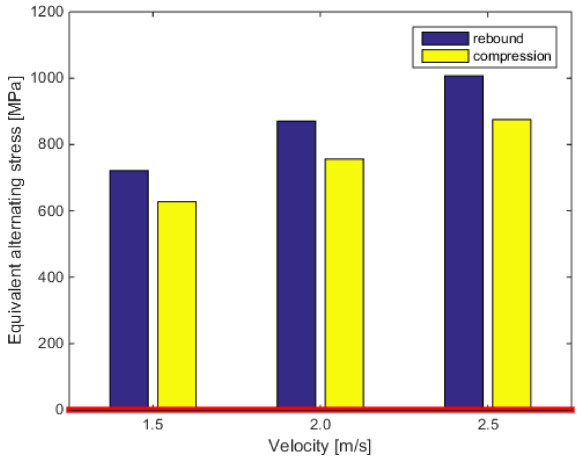

Fig. 8. Stress vs. piston-rod velocity characteristic.

The Global Optimization toolbox from Matlab package [26] was used in order to conduct the optimization. The gamultiobj solver creates a set of Pareto optima for a multi-objective minimization using the genetic algorithm [26]. The algorithm parameters, such as initial population, are automatically generated. The optima solutions were numerically obtained (Fig. 9, case #19) and then evaluated using the Minkowsky measure (Eq. (10)). The best solutions from the Minkowsky measure perspective are reported in Table 6.

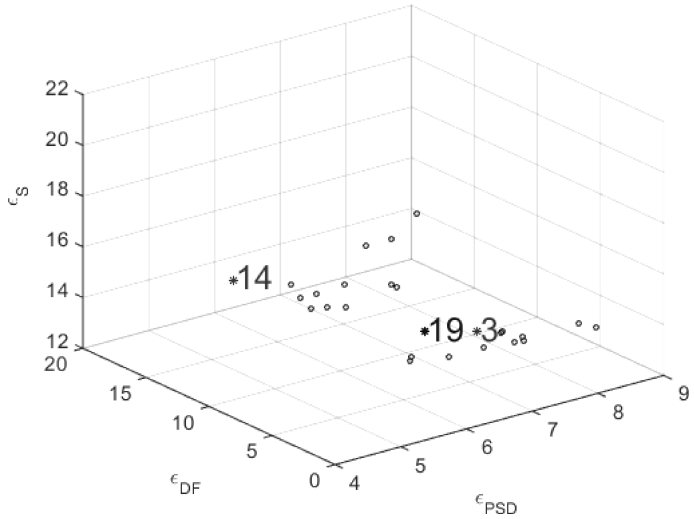

Fig. 9. Pareto frontier and feasible solution (3D).

Table 6. Optimization parameters vs. obtained results.

	Damping force [N]	Acceleration [dB]	Stress [N/m^2]
Target value	Tables 4 and 5	0	0
Acceptable target value	Tables 4 and 5	10 dB lower than initially measured	1600
Improvement direction	↕	↓	↓
Pareto frontier	0.236	5.408	8.6

The entire set of solutions is plotted in three-dimensional space (Fig. 9) corresponding to three objective functions, and for a detailed analysis three specific cross-sections (Figs. 10–12) were

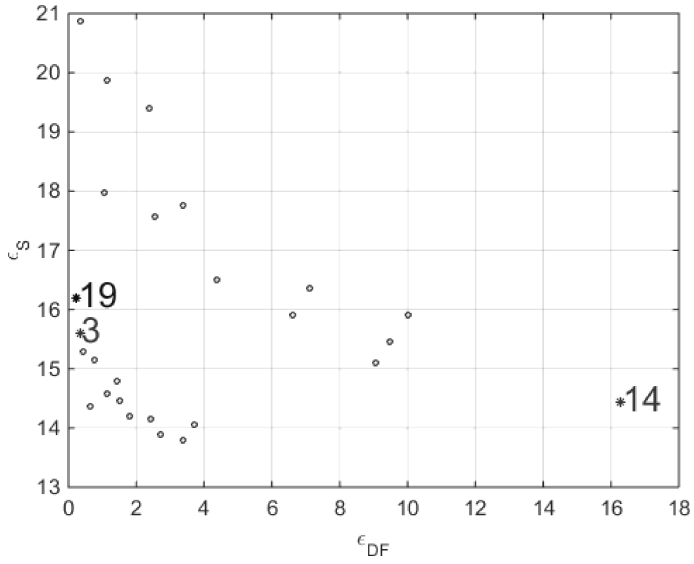

Fig. 10. Pareto frontier and feasible solution (2D).

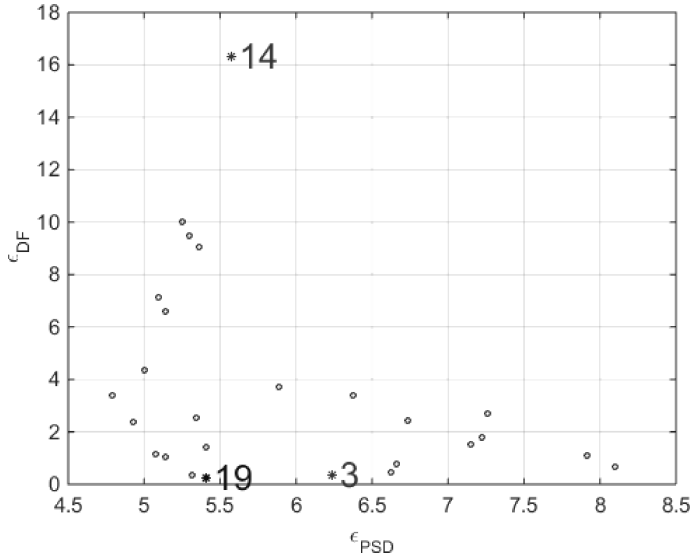

Fig. 11. Pareto frontier and feasible solution (2D).

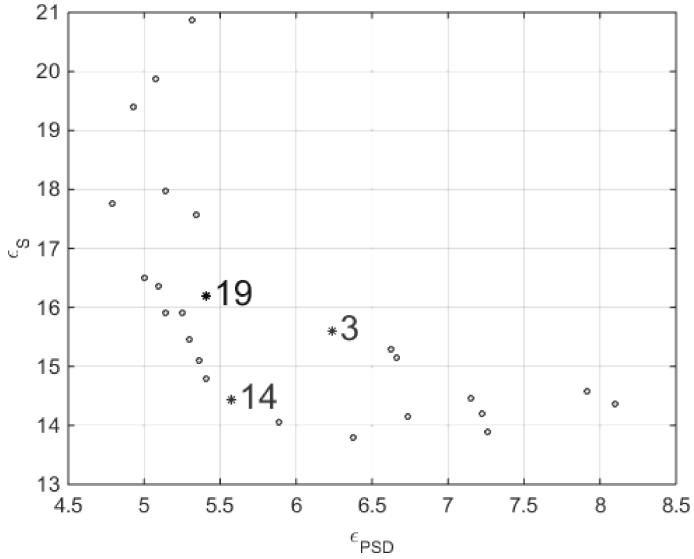

Fig. 12. Pareto frontier and feasible solution (2D).

plotted. The best identified solution (case #19) using the Minkowsky measure is indicated with a diamond marker, while other solutions (case #3) also acceptable by means of Pareto sense, are indicated with an asterisk marker.

The best setting #19, the second best setting #3, and the worst setting #14 were chosen for experimental validation and measurements regarding performance, fatigue and vibration optimization objectives.

$$X_{19} = \begin{bmatrix} 3 \\ 7 \\ 3 \\ 4 \\ 1 \\ 8 \end{bmatrix}, \qquad X_3 = \begin{bmatrix} 3 \\ 7 \\ 3 \\ 5 \\ 2 \\ 8 \end{bmatrix}, \qquad X_{14} = \begin{bmatrix} 2 \\ 7 \\ 4 \\ 8 \\ 1 \\ 8 \end{bmatrix}. \tag{15}$$

The three selected shock absorber configurations were built according to the number and thickness of discs as can be seen in Table 7 and the required top-mount force-displacement characteristics, which were ordered at the supplier.

Table 7. The parameters used to build three disc stack configurations.

Design variable	Description	Unit	#19	#3	#14
x_1	Thickness of discs for compression stroke	[mm]	0.2	0.2	0.15
x_2	Number of discs for compression stroke	[–]	7	7	7
x_3	Thickness of discs for rebound stroke	[mm]	0.2	0.2	0.25
x_4	Number of discs for rebound stroke	[–]	4	5	8
x_5	Top-mount force multiplying factor	[–]	0.1	0.2	0.1
x_6	Top-mount displacement multiplying factor	[–]	0.8	0.8	0.8

6. Validation

Performance of the three settings was evaluated with the use of the servo-hydraulic test-rig and the results of the best setting are presented in Fig. 13.

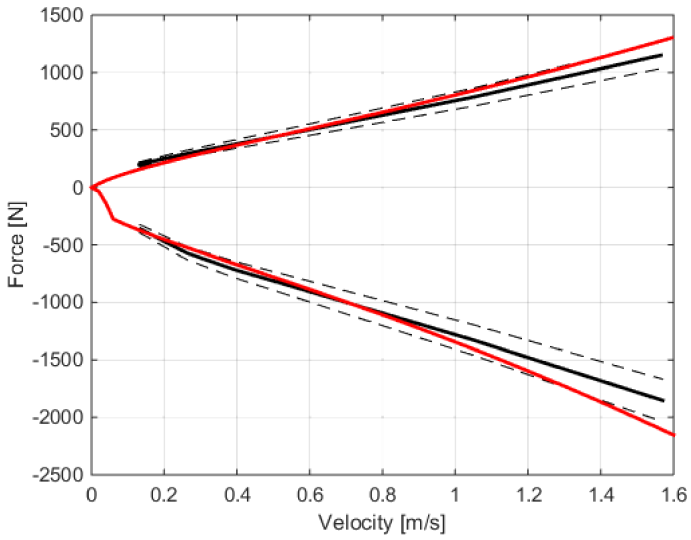

Fig. 13. Performance characteristics for Setting #19 (red line simulation, black solid line nominal reference, black dotted line upper and bottom reference band).

Damping force measurements for #19 are presented in Table 8. The case #14 does not meet the damping force MIN-MAX criteria, it is not within the force tolerance band, and therefore it cannot be accepted.

Table 8. Damping force measurements vs. simulation error.

	#19	#3	#14
Compression error (measurements vs. simulation)	16.4%	17.4%	23.2%
Rebound error (measurements vs. simulation)	9.5%	11.1%	27.9%

The overall accuracy of the damping force prediction is on a good level, as the average error does not exceed 30%. The vibration evaluation was performed using the random signal that was a narrow-band colored noise signal of the maximum peak-to-peak amplitude 10 mm. The servo-hydraulic tester was capable of transferring the random excitation to a shock absorber in the

range of 0–30 Hz and of measuring its response in the form of piston-rod acceleration in a broader range of 0–700 Hz. The wide-band vibration of a shock absorber was excited similarly to those in road conditions. The response signal was measured on the rod of the hydraulic actuator using an accelerometer. A shock absorber was rigidly attached to the main frame of the servo-hydraulic tester by means of a top fixation (the load cell) and a top mount. The bottom end of the shock absorber is connected using the bottom mount to the bottom fixation (the rod adapter) and further to the hydraulic actuator. The equivalent system of the servo-hydraulic tester is formulated as a serial connection of mass, damping, and stiffness equivalent elements. In this model, the coefficients representing damping and stiffness of a shock absorber and a hydraulic actuator are nonlinear, and their values result from the nonlinear hydraulic flow equations presented in the previous sections. The evaluation results are presented in Fig. 14.

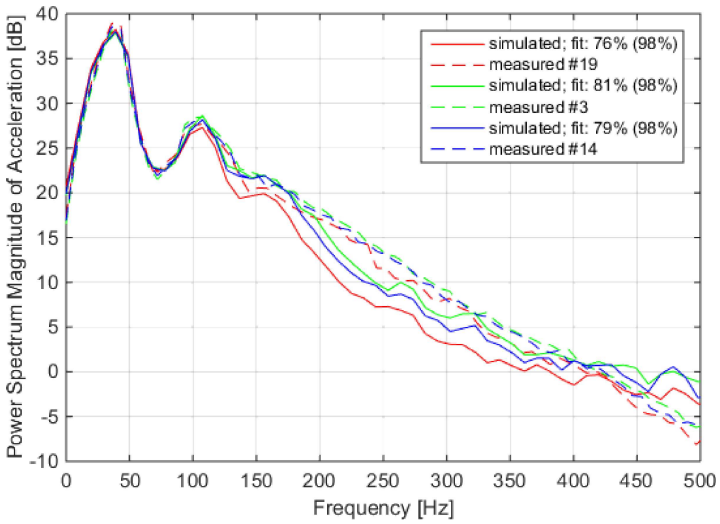

Fig. 14. Performance vibration characteristics for settings #19, #14, and #3.

The experimental results clearly show correlation between the measured and simulated shock absorber configurations. The vibration level is improved by about 2–3 dB at the frequencies of 80–120 Hz comparing settings #19 and #14, and #3 (Fig. 14). This is the most perceived frequency range by drivers and it carries more energy than higher frequency range (>120 Hz). The measurements are compared to simulation results using a percentage fit measure (i.e., normalized mean square error) and a correlation coefficient indicated by a number in brackets (Fig. 14). The influence of a shock absorber is more significant below <120 Hz, while the influence of test rig dominates >120 Hz and the measured amplitude-frequency characteristics are similar.

The stress cannot be directly measured inside the shock absorber during its operation. Nevertheless the total unit durability can be evaluated using a fatigue evaluation based on the component level tests introduced in [21]. It is important to validate how many cycles withstand the valve system in real-life scenarios. In order to characterize the sensitivity to fatigue relationship, a large number of disc stacks were tested at continuous sinusoidal cycling with constant amplitude and frequency of the applied force until the valve system damage occurs [21]. In Fig. 15, the test result reflects the number of cycles that a single valve disc is capable of withstanding [21].

The critical stress values have to be further converted into critical fatigue values using the s–N curve (Fig. 15) obtained based on the previous internal tests discussed in [21]. The stress can be converted to fatigue domain (number of cycles) using the following rules:

- the highest thickness in the disc stack dominates and it is critical,
- the most loaded and stressed valve system is critical,
- the highest velocity is critical since it provides the most demanded load conditions.

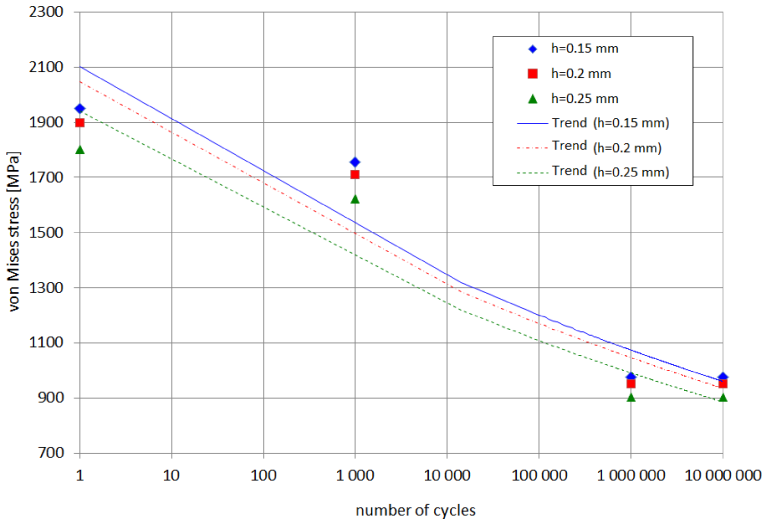

Fig. 15. Experimental s–N curve (horizontal axis has a logarithmic scale).

These rules mean, for example for #19, that the highest stress is at the rebound valve, and the greatest stress value in the rebound valve setting is at the disc of thickness h = 0.2 mm and this disc has to be considered as the weakest one (Table 9). The obtained life-times of the valve settings regarding the introduced rules are shown in Table 9.

Table 9. Parameters of the valve systems.

Description	Symbol	Unit	#19	#3	#14
Thickness of discs for compression stroke	h	[mm]	0.2	0.2	0.15
Number of discs for compression stroke	N/A	[–]	7	7	7
Thickness of discs for rebound stroke	h	[mm]	0.2	0.2	0.25
Number of discs for rebound stroke	N/A	[–]	4	5	8
Max. stress compression at 2.5 m/s	σ	[MPa]	875	876	878
Max. stress rebound at 2.5 m/s	σ	[MPa]	1007	938	804
Total critical stress at 2.5 m/s	σ_{critical}	[MPa]	1007	938	878
Total critical fatigue at 2.5 m/s	n_{critical}	[in mln. cycles]	>1	>10	>10

It is important to mention that the setting #19 is the most preferable as discs of the same thickness were indicated (standardization principle) and, in total, the number of required discs is only 11 compared to 15 for setting #14 (low cost principle). The durability of the setting #19 is, however, the lowest regarding the number of discs. This is, nevertheless, not critical as the critical fatigue is around the endurance limit. Therefore, the strength is almost not limited. However, 1 million cycles is enough for typical operational conditions since a high velocity v = 2.5 m/s rarely occurs.

7. Summary

This paper proposes and demonstrates a model-based approach toward trade-off among automotive hydraulic shock absorber design features. The fundamental challenge in a hydraulic shock absorber design process is to find the trade-off among the damping force, NVH and durability performance requirements. The multi-objective optimization method was applied based on the Global Optimization toolbox from Matlab package. Three optimization objective functions were formulated to

provide a Pareto diagram and to find the preferred solutions. The optimization results were evaluated with Minkowsky measure to determine the preferable solutions. All solutions were presented with the use of a multidimensional Pareto frontier.

The proposed model-based optimization method was validated to show its relevance in modern design approach to automotive shock absorbers. It was shown that a multi-objective approach allows including important design aspects, i.e., the damper hydraulic geometry and valve mechanical and hydraulic properties. The chosen solutions (shock absorber configurations) were further converted into a physical experiment in order to validate the optimization procedure and the shock absorber model. The experimental shock absorber was case by case equipped with the best (#19), the second best (#3) and the worst valve configuration (#14) and customized top-mounts. The validation settings are listed in Table 9.

The validation process showed that the measured damping forces were in the predicted range with the error between the model response and measurements of less than 30%. The model response was also in qualitative correlation with the measurements.

References

[1] J. Dixon. *The Shock Absorber Handbook*. John Wiley & Sons, 2008.

[2] W. Wang, X. Yang, G. Xu, Y. Huang. Multi-objective design optimization of the complete valve system in an adjustable linear hydraulic damper. *Proceedings of the Institution of Mechanical Engineers, Part C: Journal of Mechanical Engineering Science*, **225**(3): 679–699, 2011.

[3] M. Kaldas, K. Çalışkan, R. Henze, F. Küçükay. Optimization of damper top mount characteristics to improve vehicle ride comfort and harshness. *Shock and Vibration*, vol. 2014, 2014.

[4] N.V. Satpute, S. Singh, S. Sawant. Fluid flow modelling of a fluid damper with shim loaded relief valve. *International Journal of Mechanical Engineering*, **2**(1): 65–74, 2013.

[5] R. Sonnenburg. Optimized parameter combinations of hydraulic damper modules. *Journal of Transportation Technologies*, **4**(3): 277, 2014.

[6] P. Czop, D. Sławik, P. Śliwa. Static validation of a model of a disc valve system used in shock absorbers. *International Journal of Vehicle Design*, **53**(4): 317–342, 2010.

[7] P. Czop, D. Sławik. A high-frequency first-principle model of a shock absorber and servo-hydraulic tester. *Mechanical Systems and Signal Processing*, **25**(6): 1937–1955, 2011.

[8] S. Subramanian, R. Surampudi, K. Thomson. Development of a Nonlinear Shock Absorber Model for Low-Frequency NVH Applications. *SAE SP*, pp. 79–84, 2003.

[9] G. Wszołek [Ed.], P. Czop, D. Gąsiorek, J. Gniłka, D. Jakubowski, D. Sławik, J. Świder. *The Simulation Model of Hydraulic Damper for the Rapid Prototyping Needs* [in Polish: *Model symulacyjny tłumika hydraulicznego na potrzeby szybkiego prototypowania*]. Silesian Technical Univerisity, 2013.

[10] G. Kost, P. Czop, D. Jakubowski, S. Damian, T. Włodarczyk, G. Wszołek. *Parameter Estimation of First-Principle Models Formulated Using Nonlinear Ordinary Differential Equations.* Monograph. Silesian Technical University, 2013.

[11] P. Czop, D. Sławik, G. Wszołek. Development of an optimization method for minimizing vibrations of a hydraulic damper. *Simulation*, **89**(9): 1073–1086, 2013.

[12] T. Amago. Sizing optimization using response surface method in FOA. *R&D Review of Toyota CRDL*, **37**(1): 1–7, 2002.

[13] C.J. Wu, M.S. Hamada. *Experiments: Planning, Analysis, and Optimization*, *vol. 552*. John Wiley & Sons, 2011.

[14] A. Król, G. Wszołek, P. Czop. Optimization of pneumatic actuators with the use of design for Six Sigma methodology. *Journal of Achievements in Materials and Manufacturing Engineering*, **47**(2): 205–210, 2011.

[15] P. Czop, D. Sławik, T. Włodarczyk, M. Wojtyczka, G. Wszołek. Six Sigma methodology applied to minimizing damping lag in hydraulic shock absorbers. *Journal of Achievements in Materials and Manufacturing Engineering*, **49**(2): 243–250, 2011.

[16] G. Wszołek, M. Hetmańczyk, D. Sławik, P. Czop. Device for testing static and dynamic fatigue strength of valves built on the basis of disk springs. Silesian Technical University, *Patent request*, PL 407554 A1; ISSN 0137-8015; no. 20, p. 34, 2015.

[17] G. Wszołek, M. Hetmańczyk, T. Włodarczyk, D. Jakubowski, P. Czop. Active hydraulic suppressor, preferably for tuning of components and testing of the impact of the working fluid aeration phenomenon. Silesian Technical University, *Patent request*, PL 407552 A1; ISSN 0137-8015; no. 20, pp. 27–28, 2015.

[18] P. Czop, G. Kost, D. Sławik, G. Wszołek. Formulation and identification of first-principle data-driven models. *Journal of Achievements in Materials and Manufacturing Engineering*, **44**(2): 179–186, 2011.

[19] P. Czop, D. Sławik, G. Wszołek. Demonstration of first-principle data-driven models using numerical case studies. *Journal of Achievements in Materials and Manufacturing Engineering*, **45**(2): 170–177, 2011.
[20] G. Wszołek, P. Czop, A. Skrobol, and D. Sławik. A nonlinear, data-driven model applied in the design process of disc-spring valve systems used in hydraulic dampers. *Simulation*, **89**(3): 419–431, 2013.
[21] J. Świder, G. Wszołek, P. Czop, D. Jakubowski, D. Gąsiorek, D. Sławik, A. Skrobol, T. Włodarczyk, Z. Buliński, J. Gniłka. *Model-based approach applied in optimization of hydraulic valve systems*. Wydawnictwo Pracowni Komputerowej Jacka Skalmierskiego, 2013.
[22] P. Czop, D. Sławik, P. Śliwa, G. Wszołek. Simplified and advanced models of a valve system used in shock absorbers. *Journal of Achievements in Materials and Manufacturing Engineering*, **33**(2): 173–180, 2009.
[23] S.S. Rao. *Engineering Optimization: Theory and Practice*. John Wiley & Sons, 2009.
[24] M.J. Reddy, D.N. Kumar. Optimal reservoir operation using multi-objective evolutionary algorithm. *Water Resources Management*, **20**(6): 861–878, 2006.
[25] P. Czop, G. Wszołek. Model-based design approach to reducing mechanical vibrations. *Journal of Achievements in Materials and Manufacturing Engineering*, **60**(1): 39–47, 2013.
[26] MathWorks, *Global Optimization Toolbox User's Guide*. Natick 2015, 2015.